

0-----

44 articles in this issue

### A Simple Physical Model of Nonlinear Dependence of Helium Stopping Power on the Velocity of Low-Energy Hydrogen Ions

0.75 0.25 0.25 0.25

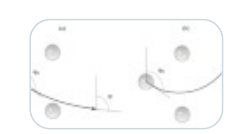
OriginalPaper | 10 September 2025 | Pages: 273 - 275

#### Mechanisms of the Volume Capture of Fast Charged Particles in a Curved Single Crystal



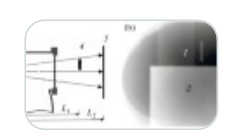
OriginalPaper | 10 September 2025 | Pages: 276 - 284

## On the Features of the Formation of Polar Distribution of Sputtered Atoms in the MD Model of the (001) Ni Face Sputtering



OriginalPaper | 10 September 2025 | Pages: 285 - 289

## Anomaly in the Interaction between Microfocus Bremsstrahlung from a New 18 MeV Betatron-Based Source and a Sharp Edge of a Steel Plate



OriginalPaper | 10 September 2025 | Pages: 290 - 295

#### **Modification of Bentonite Properties with Iron Oxide Nanoparticles**



OriginalPaper | 10 September 2025 | Pages: 296 - 303

# Study of Radiation Resistance of Optical Properties of ZrO<sub>2</sub> Micropowder Modified with MgO Nanoparticles



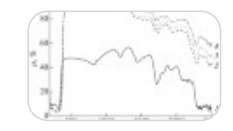
OriginalPaper | 10 September 2025 | Pages: 304 - 308

## Study of Silicon Amorphization by Xenon Ions Using Transmission Electron Microscopy and Monte Carlo Simulation



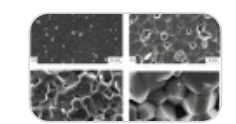
OriginalPaper | 10 September 2025 | Pages: 309 - 313

### Influence of UV and Visible Radiation on Optical Properties of Coatings Based on Two-Layer Hollow Particles of Silicon Dioxide and Zinc Oxide



OriginalPaper | 10 September 2025 | Pages: 314 - 319

#### Action of a High-Power Ion Beam of Nanosecond Duration on Commercial AIN Ceramics



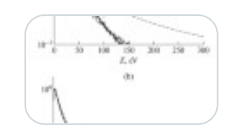
OriginalPaper | 10 September 2025 | Pages: 320 - 323

# <u>Change in the Charge State of MOS Structures under Radiation and High-Field Injection</u> at a Constant Voltage



OriginalPaper | 10 September 2025 | Pages: 324 - 328

### **Energy Spectra of Atoms Sputtered by Low-Energy Ions: Computer Simulation**



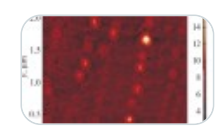
OriginalPaper | 10 September 2025 | Pages: 329 - 333

# Calculation of Binding Energy in a Fragment of a Teflon Molecule Using Density Functional Theory



OriginalPaper | 10 September 2025 | Pages: 334 - 338

# On the Use of Underwater Plasma and Magnetic Pulse Treatment of FeSiBNb Ribbon Amorphous Alloys



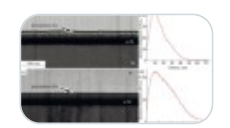
OriginalPaper | 10 September 2025 | Pages: 339 - 344

## A Study of Elastic Light-Emitting Diode Based on CsPbBr<sub>3</sub> Perovskite Film Crystallized on a Gallium Phosphide Nanowires Array



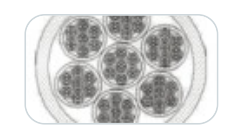
OriginalPaper | 10 September 2025 | Pages: 345 - 353

#### Initiation of Periodic Relief Development on the Silicon Surface under Ion Irradiation



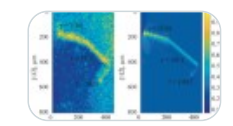
OriginalPaper | 10 September 2025 | Pages: 354 - 357

## <u>Diversity of Different-Scale Atomic Groups in a Cu–NbTi Composite under the Influence</u> of Batch Hydroextrusion



OriginalPaper | 10 September 2025 | Pages: 358 - 364

### Contemporary Phase and Achievements of the X-ray Computer Diffraction Microtomography



OriginalPaper | 10 September 2025 | Pages: 365 - 369

<u>Tribological Properties of Steel Surface in the Presence of Thermolysis Products of Nickel and Zinc Carboxylates Based on Substituted Aromatic Acids</u>



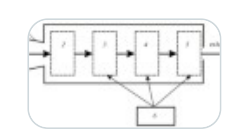
OriginalPaper | 10 September 2025 | Pages: 370 - 376

#### Etching Tracks of Swift Heavy Ions as a Tool for Creating Elongated Nanopores in Olivine



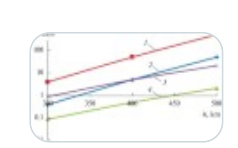
OriginalPaper | 10 September 2025 | Pages: 377 - 381

## Method for Modeling Free Molecular Flow in the Presence of Particle Sources Inside the Computational Domain



OriginalPaper | 10 September 2025 | Pages: 382 - 389

## Study of the Force Impact on the Surface of a Space Debris Object during Its Noncontact Removal from Orbit



OriginalPaper | 10 September 2025 | Pages: 390 - 398

## Structural Evolution of Nanoscale Ferroelectric $Hf_{0.5}Zr_{0.5}O_2$ Layers as a Result of Their Cyclic Electrical Stimulation



OriginalPaper | 10 September 2025 | Pages: 399 - 404

Structural Analysis of Brazilian Graphite by X-ray Diffraction, Scanning Electron

Microscopy, and Thermogravimetric Analysis with Simultaneous Differential Scanning

Calorimetry



OriginalPaper | 10 September 2025 | Pages: 405 - 412

**Crystallographic Theory of Martensitic Transformations** 



## <u>Device for Determining the Contour of the Visible Area of Optical Elements</u> (Contourograph)





OriginalPaper | 10 September 2025 | Pages: 419 - 426

## Two Channels of Minority Charge Carriers Recombination in a Homogeneous Semiconductor Target



OriginalPaper | 10 September 2025 | Pages: 427 - 432

## The Role of Electrostatic Field in the Appearance of a Narrow and Dense Layer of Metal Nanoparticles near the Surface of a Metal-Containing Dielectric after Electron Irradiation



OriginalPaper | 10 September 2025 | Pages: 433 - 436

## The Effect of Irradiation with a High-Power Ion Beam on Atmospheric Oxidation of Polycrystalline Magnesium



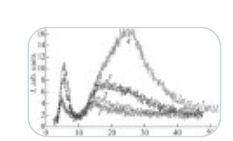
OriginalPaper | 10 September 2025 | Pages: 437 - 442

#### Modeling of Damage along the Tracks of Swift Heavy Ions in Polyethylene



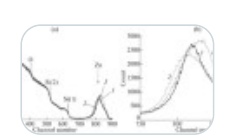
OriginalPaper | 10 September 2025 | Pages: 443 - 449

# Analysis of the Angle-Resolved X-ray Photoelectron Emission Spectra of Highly Oriented Pyrolytic Graphite



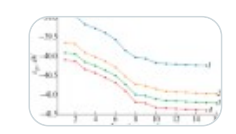
OriginalPaper | 10 September 2025 | Pages: 450 - 454

#### Study of SiO<sub>2</sub> Films Obtained by PECVD and Doped with Zn Ions



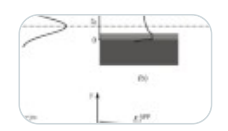
OriginalPaper | 10 September 2025 | Pages: 455 - 459

# Interpretation of X-ray Photoelectron Spectra of Ge(111), $GeO_2/Ge(111)$ , and $C_{60}F_{18}/Ge(111)$ Samples Using Quantum Chemical Calculations



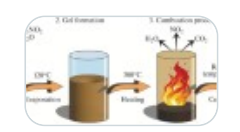
OriginalPaper | 10 September 2025 | Pages: 460 - 464

## On Optimal Conditions for Generation of Terahertz Surface Plasmon-Polaritons by the End-Fire Coupling Technique



OriginalPaper | 10 September 2025 | Pages: 465 - 469

#### Photocatalytic Activity of Ba-Doped BiFeO<sub>3</sub> Nanoparticles



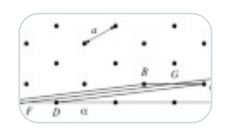
OriginalPaper | 10 September 2025 | Pages: 470 - 480

### Size Dependence of Linear Tension at a Curved Two-Dimensional Phase Boundary



OriginalPaper | 10 September 2025 | Pages: 481 - 485

## Calculation of Parameters of Electromagnetic Radiation of Accelerated Electron Beams during Sliding Interaction with a Dielectric Surface



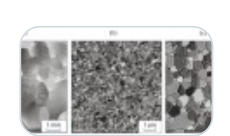
OriginalPaper | 10 September 2025 | Pages: 486 - 490

#### Change in the Free Volume in Amorphous Al<sub>88</sub>Ni<sub>10</sub>Y<sub>2</sub> Alloy under Plastic Deformation



OriginalPaper | 10 September 2025 | Pages: 491 - 496

# Structural Suppression of Blister Formation on the Surface of Tungsten under 30-keV He<sup>+</sup>-lon Implantation



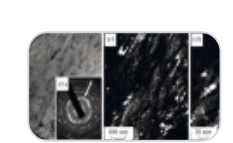
OriginalPaper | 10 September 2025 | Pages: 497 - 503

## Polymorphic States in the Electron-Beam Exposure-Induced CaSi<sub>2</sub> Film Growth at the CaF<sub>2</sub> Epitaxy on Si



OriginalPaper | 10 September 2025 | Pages: 504 - 509

## Thermal Stability of Titanium Film Formed on a Substrate by Vacuum Plasma (Argon Plasma) Electric Arc Sputtering



OriginalPaper | 10 September 2025 | Pages: 510 - 514

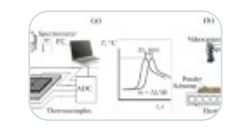
**Erosion of Aluminum-Silicon Eutectic Alloy under Compression Plasma Flows Impact** 



## Synergistic Effects of Sr-CaP and ZrO<sub>2</sub> Coatings on the Corrosion Behavior of Magnesium Alloy for Implant Applications

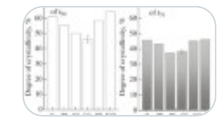
OriginalPaper | 10 September 2025 | Pages: 525 - 533

### Self-Propagating High-Temperature Synthesis in Multilayer Ti/Al/C Powder Systems



OriginalPaper | 10 September 2025 | Pages: 534 - 539

# Modification of the Structure and Elastic-Strength Properties of Elastomers Based on Nitrile Butadiene Rubber with the X-ray



OriginalPaper | 10 September 2025 | Pages: 540 - 544